2-1-1995

The Orbital Period of the Pre-Cataclysmic Binary RE 2013+400 and a Study of the Atmosphere of the DAO White Dwarf Primary

M. A. Barstow
University of Leicester

M. R. Burleigh
University of Leicester

T. A. Fleming
University of Arizona

J. B. Holberg
University of Arizona

D. Koester
Universität Kiel

See next page for additional authors

Mon. Not. R. Astron. Soc. **272,** 531–543 (1995)

The orbital period of the pre-cataclysmic binary RE 2013 + 400 and a study of the atmosphere of the DAO white dwarf primary

M. A. Barstow,[1]★ M. R. Burleigh,[1] T. A. Fleming,[2,3] J. B. Holberg,[4]★ D. Koester,[5] M. C. Marsh,[1]★ S. R. Rosen,[1] R. G. M. Rutten,[6] S. Sakai,[7] R. W. Tweedy[2] and G. Wegner[7,8,9]

[1] *Department of Physics and Astronomy, University of Leicester, University Road, Leicester LE1 7RH*
[2] *Steward Observatory, University of Arizona, 2nd & Cherry Avenue, Tucson, AZ 85721, USA*
[3] *Max-Planck-Institut für Extraterrestriche Physik, Giessenbachstrasse, D-8046 Garching, Germany*
[4] *Lunar and Planetary Laboratory, Gould–Simpson Building, University of Arizona, Tucson, AZ 85721, USA*
[5] *Institut für Theoretische Physik und Sternwarte, Universität Kiel, Germany*
[6] *Royal Greenwich Observatory/NWO-ASTRON, Apartado de Cerreos 321, E-38780 Santa Cruz de la Palma, Islas Canarias, Spain*
[7] *Department of Astronomy, Dartmouth College, Hanover, New Hampshire 03755, USA*
[8] *Astronomisches Institut, Ruhr-Universität Bochum, D-44780, Germany*
[9] *Department of Nuclear and Astrophysics, University of Oxford, Keble Road, Oxford OX1 3RH*

Accepted 1994 September 2. Received 1994 July 22; in original form 1994 May 26

ABSTRACT

Several pre-cataclysmic binaries, comprising a hot white dwarf with a red dwarf companion, have been discovered as a result of the optical identification of EUV sources from the *ROSAT* all-sky survey. The optical spectra have the steep blue continuum and Balmer absorption typical of a hot white dwarf, but there are bright, narrow emission lines of H I (and sometimes He I and Ca II) superimposed. An intense campaign of follow-up observations has been devoted to these binary systems. So far, only RE 2013 + 400 has exhibited any measurable changes in the radial velocities of the emission components, from which it is possible to estimate that the binary period is 0.71 d. A clear He II 4686-Å absorption feature is detected, which indicates that, like most PCBs with white dwarfs hotter than 40 000 K, the white dwarf is a hydrogen–helium hybrid star (DAO). A combined analysis of the optical, UV and EUV/X-ray data suggests that the atmospheric He abundance is higher in the optical line-forming region of the white dwarf photosphere than in the region where the EUV/X-ray flux is formed. This is an interesting result, in the light of the recent optical study of a sample of DAO white dwarfs by Bergeron et al., if representative of DAO white dwarfs in general.

Key words: stars: atmospheres – binaries: close – white dwarfs – ultraviolet: stars – X-rays: stars.

1 INTRODUCTION

Detached binary systems that have periods ranging from a few hours to a few days are of importance as the progenitors of cataclysmic variables (e.g. Ritter 1986). The fact that only five such systems were found among the white dwarfs in the Palomar–Green survey (Green, Schmidt & Liebert 1986) indicates that they are relatively rare. Most, if not all, of these systems must have undergone common-envelope evolution, including those with longer periods such as Feige 24 (P = 4.2 d, Thorstensen et al. 1978). Livio & Soker (1988) showed that the final separation in a system involving a supergiant may be larger than one with a giant. However, only those with sufficiently short periods or a secondary of low enough mass, about one-half of those known, will ultimately evolve to Roche lobe overflow and become cataclysmic variables (CVs) (Ritter 1986). These pre-cataclysmic systems are important, as it is possible to study each component separately, addressing questions such as how common-envelope evolution has affected the white dwarf when compared with isolated examples. It might be that individual objects have unusual chemical composition, or that the whole sample may have a different mass distribution to the isolated stars. Certainly, Feige 24 appears to have a lower

★ Guest Observer with the *International Ultraviolet Explorer.*

than average mass of 0.4 ± 0.04 $M_{\odot}$, from measurements of the gravitational redshift (Vennes & Thorstensen 1994).

The secondary star in most pre-cataclysmic systems is a red dwarf. This may be directly detectable at wavelengths beyond ≈ 5000 Å, as in, for example, the DA + dM binary RE 1629 + 781 (Cooke et al. 1992). However, often the white dwarf is particularly hot and bright, or the companion is towards the cool end of the M spectral range. In these circumstances, the only immediately apparent manifestation of the cooler star is the presence of a series of emission lines arising from the reprocessing of the white dwarf spectrum in the illuminated face of the red dwarf atmosphere or possibly from flare activity on the red dwarf (Sion et al. 1994). Examples of this are the binaries PG 1413 + 015 (Fulbright et al. 1993) and RE 1016 − 053 (Jomaron et al. 1993; Tweedy et al. 1993). The M3-5 companion in PG 1413 + 015 is only detectable directly during eclipse, although the reprocessed continuum and lines are visible at most orbital phases. In RE 1016 − 053, no continuum flux from the companion is seen out to 9000 Å. Strong H Balmer and He I lines were observed in our spectrum, but were then found to be absent some 33 d later. The strength of the emission lines is often seen to vary with orbital phase, depending on the aspect of the illuminated face of the red dwarf (see, e.g., Feige 24, Thorstensen et al. 1978).

A few of the known pre-cataclysmic systems have been found to be EUV and X-ray sources. In Feige 24, the emission appears to originate entirely from the hot H-rich DA white dwarf, which has an atmosphere containing heavy elements that suppress the emergent flux considerably at shorter wavelengths (Vennes et al. 1989). It has been speculated that these heavy elements may have originated by accretion from an M dwarf wind, but it now appears that the Feige 24 white dwarf is quite similar to other isolated DAs of the same temperature where the heavy-element opacity is a result of radiative levitation processes (Barstow et al. 1993a). In contrast, while the white dwarf in the V471 Tau system is the dominant source of EUV and X-ray emission, the K dwarf companion is also a significant X-ray source in its own right. Indeed, it is the most active coronal source in the Hyades (Barstow et al. 1992). The V471 Tau white dwarf also appears to have photospheric heavy elements (Barstow et al. 1993a), but at 35 000 K is significantly below the temperature at which the radiative levitation mechanism becomes efficient (40 000–50 000 K, e.g. Vauclair 1989; Chayer, Fontaine & Wesemael 1991). However, there is active accretion from the K dwarf wind (Barstow et al. 1992) which could explain this anomaly.

The *ROSAT* Wide Field Camera (WFC) EUV sky survey has yielded a large number of new white dwarf detections (see Pounds et al. 1993). Approximately 50 per cent of these stars were previously uncatalogued objects, whose nature was discovered through a series of optical identification observations performed in both northern and southern hemispheres (Mason et al. 1991). The only two known pre-CV objects detected by the WFC were Feige 24 and V471 Tau, discussed above. To be visible as an EUV source, any white dwarf must satisfy several criteria. If it is a DA white dwarf, the temperature must be greater than $\approx 23\,000$ K; if it is a DO or PG 1159 star, the He must be substantially ionized before any EUV flux emerges – requiring a temperature of 70 000 K or more. In addition, there must not be too much other absorbing material present, either in the intervening interstellar medium or circumstellar material or in the form of photospheric heavy elements. Unexpectedly, many of the known pre-CV white dwarfs are DAO-type hybrid white dwarfs, DA stars containing spectroscopically detectable He II. It is notable that no isolated DAOs were detected in the survey, probably due to absorption by the photospheric He and/or heavier elements, and so it is perhaps not too surprising that those DAOs in pre-CVs were not detected either. Nevertheless, a significant number of binary systems containing a DA white dwarf plus an M dwarf were detected by the WFC and identified by the subsequent optical programme, including RE 1629 + 781 (Cooke et al. 1992), RE 1016 − 053 (Jomaron et al. 1993; Tweedy et al. 1993) and RE 2013 + 400 (Barstow et al. 1993b). Considering the above discussion, such systems must represent a special subclass of the pre-CVs in having white dwarfs that are also EUV sources. However, RE 1016 − 053 was found to be anomalous compared to other EUV detections of H-rich white dwarfs, in that it is classified as a DAO from the detection of He II λ4686. This was the first reported detection of a DAO white dwarf in the EUV. Further observations of RE 2013 + 400, discussed in this paper, reveal it also to be a DAO white dwarf.

The interpretation of the RE 1016 − 053 observations (Tweedy et al. 1993) considered the then-standard model of DAO white dwarf structure as a stratified H upon He envelope (Vennes et al. 1988). However, the small H layer mass implied by the strength of the He II line would imply an EUV opacity much greater than observed and the non-detection of the star. Hence the structure of the white dwarf in RE 1016 − 053 did not appear to be consistent with the standard DAO picture, as the He present must be more uniformly distributed in the envelope for it to be an EUV source. Subsequently, Bergeron et al. (1994) have carried out a detailed spectroscopic study of 14 DAO white dwarfs, which yields the surprising result that, in the optical line-forming region, most of these objects are not stratified after all, but are best interpreted by homogeneous compositions. Their results also suggest that most DAOs have lower masses than typical field DA white dwarfs. The main exceptions are the pre-CVs in the sample, including the two EUV detections RE 1016 − 053 and 2013 + 400, which appear to have normal masses, indicating a different evolutionary history. As Vennes et al. (1988) have demonstrated that He should sink rapidly out of a white dwarf atmosphere, some currently unidentified physical mechanism must be competing against gravitational settling. Furthermore, Bergeron et al. (1994) suggest that both RE 1016 − 053 and 2013 + 400 are detected in the EUV by virtue of lower heavy-element opacity compared to the other, mostly hotter, DAO white dwarfs.

The initial discovery of the binary nature of RE 2013 + 400 was made as part of the *ROSAT* WFC optical identification programme (see Mason et al. 1991) and reported in the *ROSAT* Wide Field Camera Bright Source Catalogue (Pounds et al. 1993). This was easily determined from the blue continuum slope of the white dwarf, together with the Balmer absorption lines from Hβ through to Hϵ. Evidence for the presence of an M dwarf companion was found in the Hα and Hβ emission lines, detectable even with the relatively low resolution (≈ 10 Å) of the Faint Object Spectrograph

(FOS) on the 2.5-m Isaac Newton telescope. The continuum of the M star could barely be distinguished, but a careful analysis of the FOS data suggests it has a spectral type between M2 and M4 (Jomaron, private communication). In carrying out a further series of optical observations on the new white dwarfs discovered by the *ROSAT* WFC, to obtain measurements of T and $\log g$ from the Balmer line profiles, we have noted that RE 2013+400 is a near-spectroscopic twin to RE 1016−053 (Barstow et al. 1993b). The He II λ4686 absorption line was clearly visible in the spectra, as were a large number of emission lines. The emission-line cores in the H Balmer series showed apparent radial velocity changes between observations made on three successive nights, indicating that the binary period is less than a day. Clearly, this is an important object for further study, and additional observations have since been carried out. We report here on a detailed analysis of the optical, UV, EUV and X-ray data that we have obtained for this source. From this, we are able to determine the temperature, gravity and photospheric He abundance of the white dwarf, to determine the binary period and estimate the masses of the components. We discuss this object in the context of its nature as a pre-CV system and as one of only two DAO white dwarfs, both in binaries, detected in the EUV and X-ray.

2 OPTICAL AND UV OBSERVATIONS

RE 2013+400 was first detected in the *ROSAT* WFC sky survey (Pounds et al. 1993). Subsequent optical spectroscopy (Barstow et al. 1993b) discovered bright Balmer series emission lines which varied in wavelength from night to night, clearly indicating that RE 2013+400 is a binary system similar to RE 1016−053 and other pre-CVs. Presently, there exists no optical photometry of RE 2013+400. However, an estimate of $V=14.6$ was made from the optical ID programme. RE 2013+400 is also present as a weak source in the *Extreme Ultraviolet Explorer* (*EUVE*) sky survey catalogues of Bowyer et al. (1994) and Malina et al. (1994). A wide variety of observations have now been made of the RE 2013+400 system. These are mainly optical, but also cover the UV, EUV and X-ray. Table 1 summarizes the type, sources and dates of these observations, which are all discussed in more detail below.

2.1 Temperature, gravity and abundance measurements

Since the discovery of many new white dwarfs with the optical identification programme, we have carried out a further set of observations with the aim of obtaining high signal-to-noise ratio spectra with 3–8 Å resolution to measure the temperature and gravity of each star, by fitting synthetic spectra to the Balmer line profiles. This work has been carried out using the Steward Observatory (SO) 2.3-m telescope in the north and the 1.9-m Radcliffe telescope of the South African Astronomical Observatory in the south. RE 2013+400 was first observed as part of this programme on 1992 July 1, using a Boller & Chivens spectrograph and a blue-sensitive TI 800×800 CCD to cover the spectral range from the Balmer limit to Hβ at approximately 8-Å resolution. The strong series of H Balmer and other emission lines immediately set this apart as a possible pre-CV type binary system (Fig. 1). Consequently, the system was also observed on the two succeeding nights (July 2 and 3, see also Fig. 1). The Balmer emission lines are visible through to H14, before becoming lost in the noise in the data, and several He I lines, Ca II K and possibly C IV are also seen. Table 2 lists the line identifications. In addition to the H Balmer absorption lines, He II λ4686 is clearly detected.

In principle, this system can be treated as a double-lined spectroscopic binary, allowing us to derive the orbital period and mass function. We discuss this in more detail in Sections 2.3 and 3, with other radial velocity data taken at a later date. It is also possible to determine the temperature and gravity of the white dwarf, using the now-standard technique of fitting the predicted Balmer line profiles from stellar model atmosphere calculations to the observational data (see, e.g., Bergeron, Saffer & Liebert 1992). We used both homogeneous and chemically stratified grids of H/He models calculated by one of us (D. Koester, see Koester 1991), spanning the temperature range 20 000–100 000 K and $\log g$ from 7.0 to 9.0. Spectral fitting was performed using the program XSPEC (Shafer et al. 1991). As the optical spectra show He II λ4686, we have allowed the He abundance and H layer mass, in the homogeneous and stratified models respectively, to vary along with T and $\log g$. We have also measured directly the equivalent width of the He II absorption feature, as a parameter which is completely independent of the spectral model. Since the absorption lines also have emission cores, we model each of these with an individual Gaussian component, whose width, amplitude and velocity are all free parameters, in the spectral fitting exercise.

In dealing with CCD spectra, where the errors on individual data points are difficult to determine, we first perform an initial fit to the data without errors included. From the scatter on the residuals between the best-fitting model and the observed spectrum, we then estimate the average errors on the data points, which are included in a

Table 1. List of observations of RE 2013+400.

Telescope	Data/Resolution	Wavelength (Å)	Dates
ROSAT WFC	broad band	60–200	October 1990
ROSAT PSPC	broad band	5–125	October 1990
2.3m SO	spectra 8Å	3500–5000	1-3 July 1992
2.5m INT + IDS	spectra 1.0Å	4000-5000	8 October 1992
IUE	SWP46426 6Å	1150-1950	8 Dec 1992 (exposure 14m)
2.4m MDM	spectra 3.5Å	5090-7050	8 May 1993

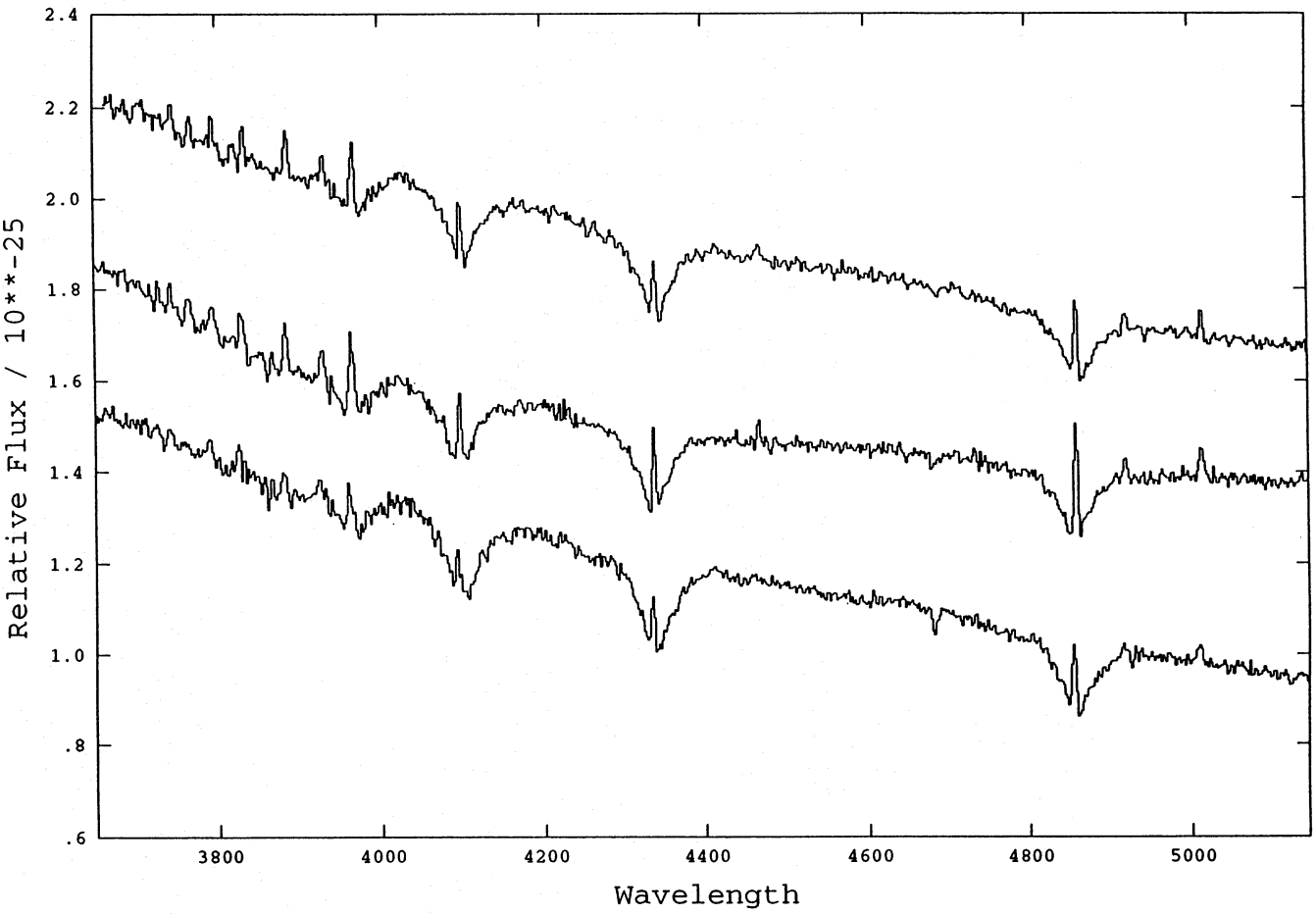

Figure 1. Three optical spectra of RE 2013+400 recorded on 1992 July 1 (bottom), 2 (centre) and 3 (top), using the 2.3-m Steward Observatory telescope. Strong Balmer and other emission lines are present in all three spectra, along with a He II 4686-Å absorption feature. Variability in the He II line strength, discussed in the text, can be seen.

Table 2. Emission lines in the RE 2013+400 spectrum.

Rest wavelength (Å)	Identification	Rest wavelength (Å)	Identification
3723	H14	4102	Hδ
3735	H13	4227	CaI
3750	H12	4340	Hγ
3770	H11	4441	CIV (weak)
3797	H10	4471/4472	HeI
3835	H9	4861	Hβ
3889	H8/HeI	4922	HeI
3934	CaII (k)	5015	HeI
3968	Hϵ	6563	Hα

subsequent fit. At the same time, we correct for any systematic deviation in the spectral slope between model and data, arising from slight errors in the flux calibration. A second spectral fit results in no change to the best-fitting parameters but, with the inclusion of errors on the data points, has a lower reduced χ^2. To make a sensible estimate of the uncertainty in the fitted parameters, the reduced χ^2 should be less than ≈ 2, and this is usually achieved with a single iteration of the steps outlined above.

Each of the three CCD spectra of RE 2013+400 were treated entirely independently in the spectral fitting exercise, which utilizes the Hβ, Hγ, Hδ and Hϵ lines. Since significant radial velocity variations are clearly seen in the system, co-addition of the spectra, to improve the signal-to-noise ratio,

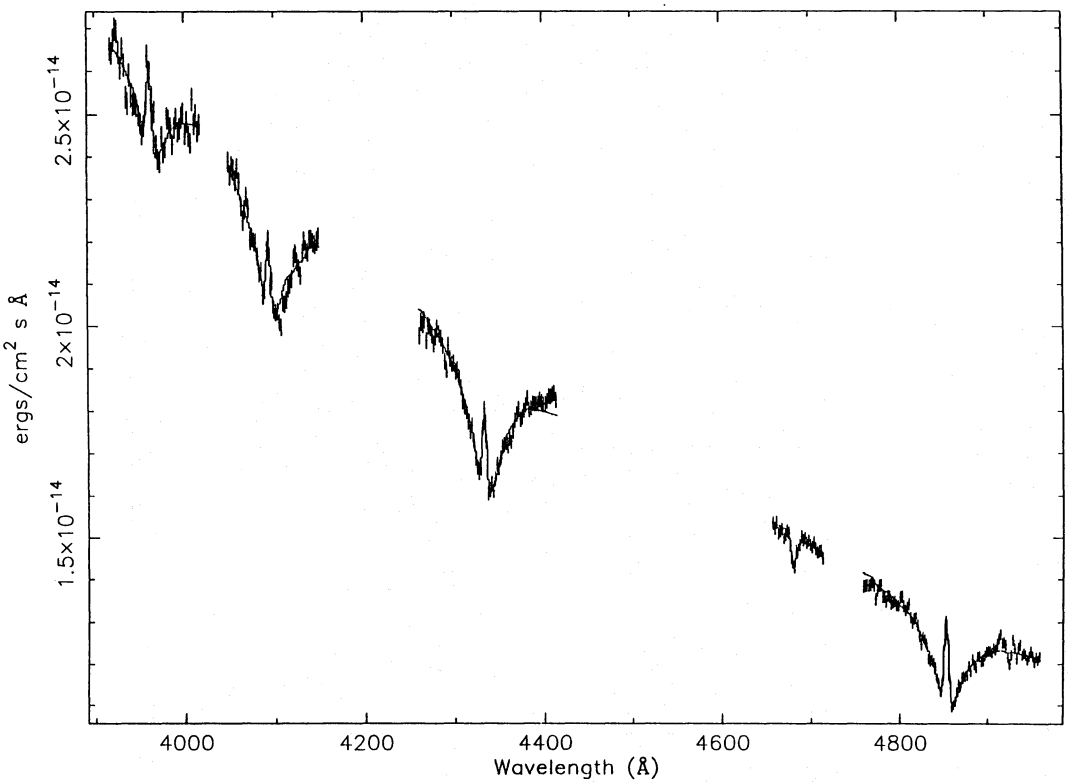

Figure 2. An example of a homogeneous model atmosphere fit to the Balmer absorption, Balmer emission and He II absorption in the July 1 spectrum. The best-fitting model has $T = 47\,200$ K, log $g = 7.99$ and log He/H = -2.7 (see Table 3).

Table 3. Best-fitting temperatures, gravities and He abundances plus He II equivalent widths for the three Steward Observatory spectra. The 90 per cent error ranges are enclosed in brackets.

Date	T (K)	log g	log He/H	HeII ew (mÅ)
1 Jul 1992	47,200 (46,000–48,000)	7.99 (7.89–8.04)	−2.71 (−2.53 to −2.88)	347 (±60)
2 Jul 1992	47,300 (46,440–48,230)	7.58 (7.49–7.68)	−3.60 (−3.37 to −3.80)	196 (±60)
3 Jul 1992	46,670 (45,680–47,690)	7.66 (7.57–7.74)	−3.29 (−3.02 to −3.51)	220 (±60)

carries the risk of artificially broadening the Balmer lines. An example of the line fits is shown for a homogeneous H + He model in Fig. 2, and the fits are of equal quality for each observation. With a stratified model the best fit to the He II 4686-Å absorption line corresponds to the thinnest H layer (1.0×10^{-15} $M_\odot$) in the stratified grid. Since the EUV and soft X-ray fluxes predicted by this model are far below the sensitivities of the *ROSAT* instruments, we do not consider the stratified models further. We also note that stratified models were ruled out by Bergeron et al. (1994) on the basis of a poor fit to the He II 4686-Å line profile. The best-fitting temperatures, gravities and He abundances (for the homogeneous models) plus the He II equivalent widths, together with their 90 per cent confidence errors, are listed in Table 3. All the temperature measurements are in good agreement, well within the uncertainties in the analysis, but, while the values of log g obtained from the July 2 and 3 data are similar, the July 1 figure is somewhat higher. In addition, the measured He abundance appears to vary from night to night. There is a corresponding variation in the He II 4686-Å line equivalent width, which indicates that this is a true change in the inferred amount of He rather than an effect of the higher value of log g obtained from the July 1 fit. A χ^2 test on these data points and associated uncertainties shows the He II equivalent width and the inferred He abundance to be variable at the 99 per cent confidence level. These changes do not necessarily arise from intrinsic variation in the photospheric content, but may be a result of infilling of the absorption feature by an emission line associated with the red dwarf. It can certainly be seen in Fig. 1 that the strength of the emission lines we have detected does change, and we note that the measured He abundance seems to be inversely correlated with this.

Using the evolutionary models of Wood (1992), we can estimate the mass and radius of the white dwarf from the optically determined T and log g. Considering the full range of uncertainty arising from the extremes of each of the three fits, we find that the mass is between 0.48 and 0.72 $M_\odot$. The corresponding radius lies in the range 0.013 to 0.022 $R_\odot$, giving an estimated distance between 95 and 155 pc.

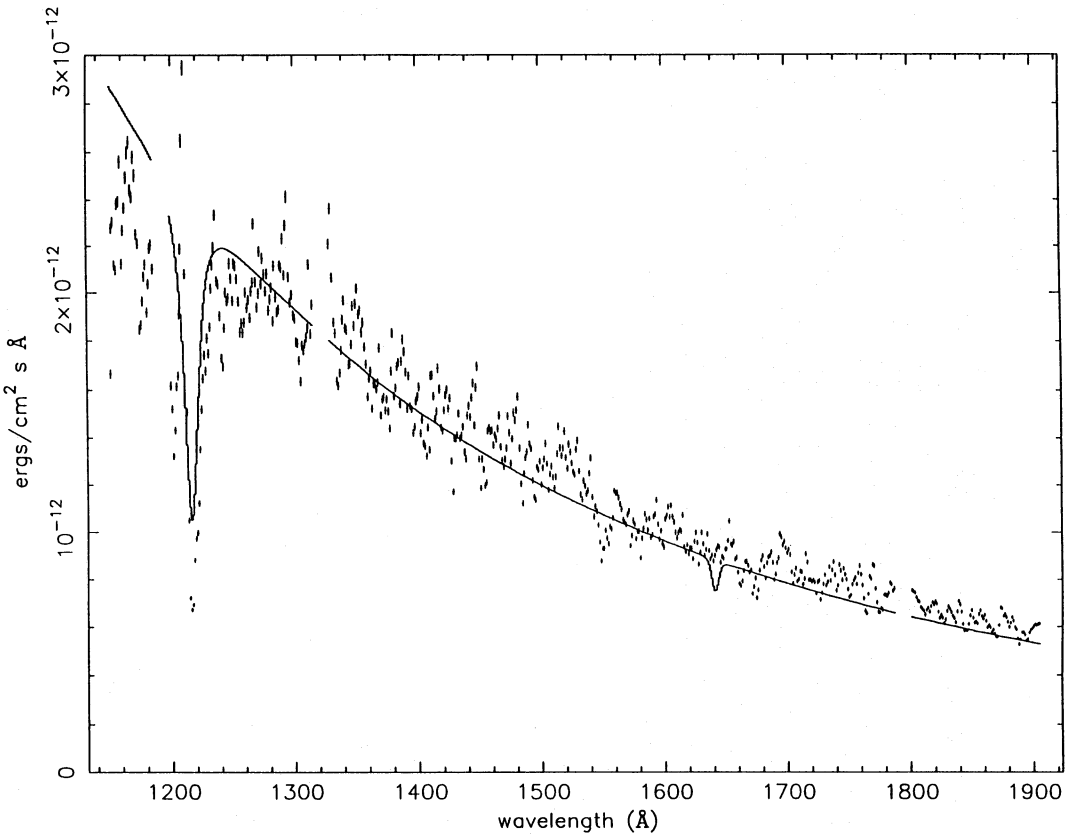

Figure 3. *IUE* SWP spectrum of RE 2013+400 (error bars) compared to a $T=47\,000$-K, $\log g=7.7$ model spectrum (continuous curve) incorporating a helium abundance at the upper limit formally allowed by the data ($\log \mathrm{He/H}=-2.5$). The gaps in the data and model correspond to reseau points.

2.2 Far-UV observations

A low-dispersion far-UV spectrum of RE 2013+400 was obtained by the *IUE* satellite on 1992 December 8. The 14-min exposure (Fig. 3) reveals strong absorption from the unresolved C IV doublet at 1550 Å with a measured equivalent width of 1600±800 mÅ. C IV was also detected in the SWP spectrum of RE 1016−053 (Tweedy et al. 1993), but at about half the strength. While the spectrum becomes noisier at shorter wavelengths, there is also a possible Si III feature at 1300 Å with an equivalent width of 1000±400 mÅ. In contrast to RE 1016−053, there is no evidence for any He II absorption at 1640 Å, which we might have expected to see given the presence of He II 4686 Å in the optical spectrum. It is possible to determine an upper limit to the He abundance allowed by the *IUE* spectrum by fitting it in the He II region with the lines in our homogeneous H+He model grid. Formal flux errors are difficult to determine for *IUE* data, due to the nature of the detector system, but examination of the point-to-point scatter in the spectrum indicates that a realistic error estimate is ±20 per cent. Fixing the temperature and gravity within the range allowed by the optical data, we obtain a 90 per cent confidence upper limit to $\log \mathrm{He/H}$ of −2.5, which is entirely consistent with the values indicated by the optical spectra. The model spectrum with $T=47\,000$ K, $\log g=7.7$ and $\log \mathrm{He/H}=-2.5$ is plotted in Fig. 3, for visual comparison with the data.

2.3 Radial velocity and emission-line strength variations

It is apparent, from a cursory examination of the spectra in Fig. 1, that RE 2013+400 exhibits substantial radial velocity variations, the emission lines changing position with respect to the cores of the absorption features. These data were each taken 24 h apart, and do not sample the orbital phase very well. Furthermore, the wavelength, and therefore the velocity, scales are not well calibrated. Additional observations were obtained as part of the service programme of the Isaac Newton 2.5-m telescope (INT) in 1992 October (Observer RGMR), using the Intermediate Dispersion Spectrograph and an EEV blue-sensitive CCD. These spectra span a wavelength range of 4000 to 5000 Å at a resolution of 1 Å, encompassing Hδ through to Hβ, and a time period of ≈3 h. Further spectra were also taken at the Michigan–Dartmouth–MIT 2.4-m telescope by one of us (SS) in 1993 May, using the Mark III spectrograph with a 600 line mm^{-1} grism and an unthinned Loral 2048×1048 CCD. Once again the spectra cover about 3 h, but on this occasion the data only included Hα. The instrument resolution was 3.5 Å. Figs 4(a) and (b) show examples of the INT and MDM spectra, which were not flux-corrected in either observing run.

With the SO and INT data sets it is possible to obtain both velocity measurements, from the emission lines for the red dwarf, and from the absorption lines for the white dwarf. As the Balmer absorption lines are considerably broader

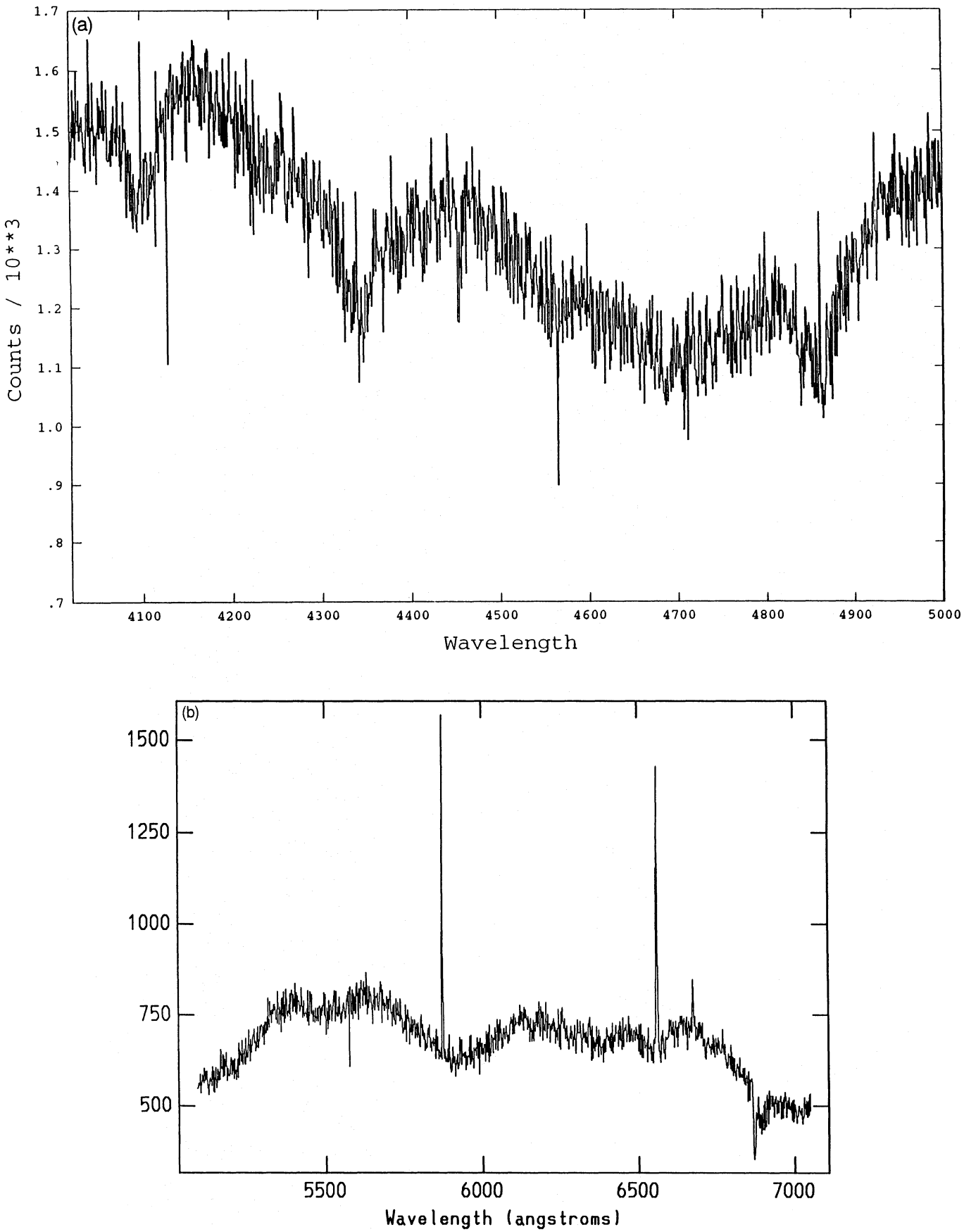

Figure 4. (a) One of the seven optical spectra spanning Hβ, Hγ and Hδ lines recorded with the 2.5-m Isaac Newton telescope and IDS. (b) An example of the Hα region spectra recorded using the MDM 2.4-m Hiltner telescope.

than the emission features, the errors in the velocity determination are considerably larger – ≈ 150 km s^{-1} compared with 30 km s^{-1}. Of the absorption lines, the He II feature is the narrowest, and so it is probably the most reliable determination of the velocity of the white dwarf, giving an error between 50 and 100 km s^{-1} depending on the equivalent width of the line. Unfortunately, the signal-to-noise ratio of the INT data is somewhat lower than that of the SO spectra, and the He II line is not reliably detected in all these. We have adopted the following approach in this analysis. In all three data sets the emission lines were modelled by Gaussian profiles, and the velocity shifts of the lines were determined in the usual way by comparing the observed wavelength of each feature with the rest wavelength. An equivalent width was also obtained for each line. Only Hβ is clearly detected in all the INT spectra and only Hα is present in the MDM data, so we have chosen to make use of the Hβ line alone from the SO observations. While it is feasible to assemble the velocity observations for different lines into a coherent list, it is clearly inappropriate to compare equivalent widths for the different lines. Consequently, we concentrate our analysis of the line-strength variations on Hβ, the line for which we have most data.

As mentioned above, the velocity scale for the SO data is very uncertain, changing by 100–200 km s^{-1} between each night. However, since we have velocity measurements for both stars in the system and an estimate of the mass of the white dwarf (see Section 2.1), it is possible to determine a velocity range for the centre of mass from the range of possible M dwarf masses (0.2–0.4 $M_\odot$). The measured velocities can then be corrected to the centre-of-mass frame, provided that an error, arising from the uncertainty in the position of the centre of mass, is included in addition to the formal measurement errors. Finally, we estimate the absolute velocity of the centre of mass from those INT data where both He II absorption and Hβ emission velocities can be obtained. The cumulative errors on the SO data velocities are substantial compared with the formal measurement errors but, given their time spacing compared to the INT and MDM data, they are important for resolving possible aliases in the period determination. Table 4 summarizes all the radial velocity measurements, equivalent widths and associated errors, after comparison with radial velocity standards and correction for the space motion of the Earth with respect to the line of sight.

3 ORBITAL PARAMETERS OF THE SYSTEM

We have determined the binary orbital period of the system by fitting a sine wave to the measured radial velocities of the emission lines. The implicit assumption that the orbit is circular is reasonable, since the magnitude of the velocity

Table 4. Radial velocities for Hβ or Hα emission, equivalent widths (ew) for Hβ emission, and He II velocities and equivalent widths.

MJD	emission		HeII absorption	
	Velocity (km s^{-1})	ew (mÅ)	Velocity (km s^{-1})	ew (mÅ)
48804.3067	-134 ± 40	970 ± 15	-26 ± 64	350 ± 60
48805.3686	42 ± 45	1579 ± 15	-147 ± 100	200 ± 60
48806.3986	-93 ± 32	1171 ± 15	-97 ± 77	220 ± 60
48903.8609	-92 ± 23	768 ± 20	-181 ± 120	350 ± 100
48903.8727	-77 ± 15	485 ± 20	-32 ± 120	280 ± 60
48903.8890	-38 ± 82	472 ± 20	—	—
48903.9388	-29 ± 25	252 ± 20	—	—
48903.9528	-7.8 ± 19	392 ± 20	-106 ± 84	450 ± 50
48903.9641	8.0 ± 19	388 ± 20	-183 ± 84	440 ± 50
48903.9756	8.3 ± 22	450 ± 20	-69 ± 280	330 ± 70
49115.3646	-109 ± 20			
49115.3754	-95 ± 20			
49115.3858	-102 ± 20			
49115.3997	-87 ± 20			
49115.4108	-98 ± 20			
49115.4226	-102 ± 20			
49115.4379	-86 ± 20			
49115.4490	-96 ± 20			
49115.4601	-95 ± 20			
49115.4733	-78 ± 20			

changes already indicates that the period is ≈ 1 d or less, and therefore that the system has undergone a period of common-envelope evolution which would have circularized the orbit. The best fit ($\chi^2 = 3.9$, 17 degrees of freedom) gives a period (P) of $0.710\,13 \pm 0.000\,20$ d, a velocity semi-amplitude ($v \sin i$) of 85 ± 26 km s^{-1}, and a systemic velocity of -19 ± 19 km s^{-1}. We note that this value for $v \sin i$ is much lower than an earlier estimate (Barstow et al. 1993b), derived from just two of the SO spectra. Sine fits to possible alias periods produce substantially higher values of χ^2 (e.g. 35.7 for $2P$ and 16.4 for $0.5P$). Application of the F-test to these and the best-fitting χ^2 allows us to discount these alternative periods (and indeed all others) with a confidence greater than 99 per cent. We note that our results are in agreement with other measurements briefly reported by Thorstensen & Vennes (1994).

Fig. 5 shows all the measured parameters – emission-line velocity, Hβ equivalent width, He II velocity and He II equivalent width (in Figs 5a, b, c and d, respectively) – folded by the measured period with zero phase corresponding to MJD 48803.5. The combined data sets sample just over half a binary cycle and, as shown in Fig. 5(b), do not cover the maximum in the Hβ equivalent width variation. However, it is clear that the Hβ equivalent width minimum occurs 0.25 cycles (phase 0.45) before the velocity maximum, i.e. when the emission source is at inferior conjunction. This is expected if the line emission arises from reprocessing of the EUV radiation from the white dwarf incident on the inward face of the red dwarf. The maximum emission should occur at superior conjunction, 0.25 cycles after the velocity maximum (phase 0.95), where we have no data.

In principle, it is possible to use the He II absorption-line velocity amplitude in association with the known limits on the white dwarf and red dwarf masses to determine a complete orbital solution (separation and inclination) for the system. Unfortunately, the errors on the He II velocity changes are large (see Fig. 5c). A sine fit to the folded data yields a semi-amplitude in the range 0 to 63 km s^{-1}. Kepler's third law gives the separation a (in solar radii),

$$a \approx 0.5\ \mathrm{R}_\odot m^{1/3} P^{2/3}$$

(see, e.g., King 1989), where m is the total mass in solar units, and P is in hours. The possible range of the total mass is 0.68 to 1.12 $\mathrm{M}_\odot$, implying a separation between 2.9 and 3.4 $\mathrm{R}_\odot$. Since $a = vP/\pi$ (v is the orbital velocity) the inclination of the system can be estimated directly from the observed $v \sin i$. With the large uncertainties in the velocity semi-amplitude of the white dwarf, $v \sin i$ can range from 80 to 178 km s^{-1}, the lower limit being imposed by the upper limit on the white dwarf/red dwarf mass ratio rather than the velocity measurements. Consequently, the lower limit to the inclination of the system is 40°, with the upper limit being 90°.

A comparison of Figs 5(b) and (d) illustrates the anticorrelation between the depth of the He absorption and the strength of the Hβ emission line, to which we drew attention in Section 2.1. A plausible explanation for this effect is that the He II absorption feature is being partially filled by an He II emission component associated with the red dwarf, with a strength varying in phase with the Hβ line. Within the errors, the maximum equivalent width corresponds to a measured value of log He/H of ≈ −2.6. Whether or not this represents the true He abundance we cannot determine, since we have no way of independently measuring the possible contribution from any He II emission. Consequently, we can only treat this as a lower limit to the abundance of He in the star.

4 ANALYSIS OF THE EUV AND X-RAY DATA

The reduction and analysis of *ROSAT* observations of white dwarfs have been discussed extensively in several earlier papers (e.g. Barstow et al. 1993a, 1994); hence we include only the briefest details here. The *ROSAT* survey data consist of three broad-band data points – WFC S2 (114–200 Å), WFC S1 (60–140 Å) and the PSPC (25–100 Å). The measured count rates (count s^{-1}), after correction for changes in the instrument response during the survey, are 0.033 ± 0.006, 0.062 ± 0.007 and 0.935 ± 0.034, respectively. Since the RE 2013+400 white dwarf is a member of a binary system, we must consider whether or not any of the observed EUV/X-ray flux can be attributed to the M dwarf. In the energy range covered by the PSPC, the flux from even the hottest white dwarfs lies longward of the carbon K edge in the counter window (at 44.7 Å). Hence the detected emission from RE 2013+400, at 0.038 ± 0.010 count s^{-1}, shortward of this wavelength must be from the M dwarf, and some estimate of the contribution in the longer wavelength bands must be made. A useful comparison can be made between this system and the DA+dK binary V471 Tau. The primary in V471 Tau is extremely active, yet contributes only ≈ 20 per cent of the flux in the longer wavelength PSPC band and nothing measurable in the EUV (Barstow et al. 1992). Since the RE 2013+400 white dwarf is substantially hotter than that in V471 Tau (35 000 K), the fraction of the PSPC long-wavelength flux arising from the white dwarf should be larger. The red dwarf in RE 2013+400 appears to be a dMe star, although a significant fraction of the Balmer line fluxes is associated with reprocessed radiation from the white dwarf rather than intrinsic dMe-like activity. Fleming et al. (1994) find that a typical dMe count rate ratio, in long- and short-wavelength PSPC bands, is 2 to 1. Taking this as representative of the red dwarf in RE 2013+400, we estimate that the count rate from the white dwarf has a lower limit of 0.86 count s^{-1}. We take this into account in our subsequent analysis, where the observations are compared with the predictions of our H+He model atmospheres using XSPEC but, as we do not have an accurate V magnitude for the white dwarf in the system, the models were normalized using the flux measured at 1400 Å with *IUE*. Temperature and gravity were allowed to vary within the ranges covered by the optical analysis.

With a stratified model, to fix the H layer mass at the lower limit of the grid ($1.5 \times 10^{-15}\ \mathrm{M}_\odot$), as required by the strength of the He II 4686-Å feature (see Section 2.1), gives predicted count rates in S1 and the PSPC that are three orders of magnitude below the observed values when the interstellar column is adjusted to fit the S2 count rate. Hence we can categorically rule out the possibility that RE 2013+400 has a stratified atmosphere. In studying the homogeneous composition models, two approaches were taken. First, the He/H abundance was fixed at the lower limit allowed by the optical data (log He/H = −2.7). The best fit to the data ($T = 45\,680$ K, log $g = 7.66$) yields a reduced χ^2 of 20, well outside any reasonable confidence limits. Although the S2 count rates are in good agreement, the

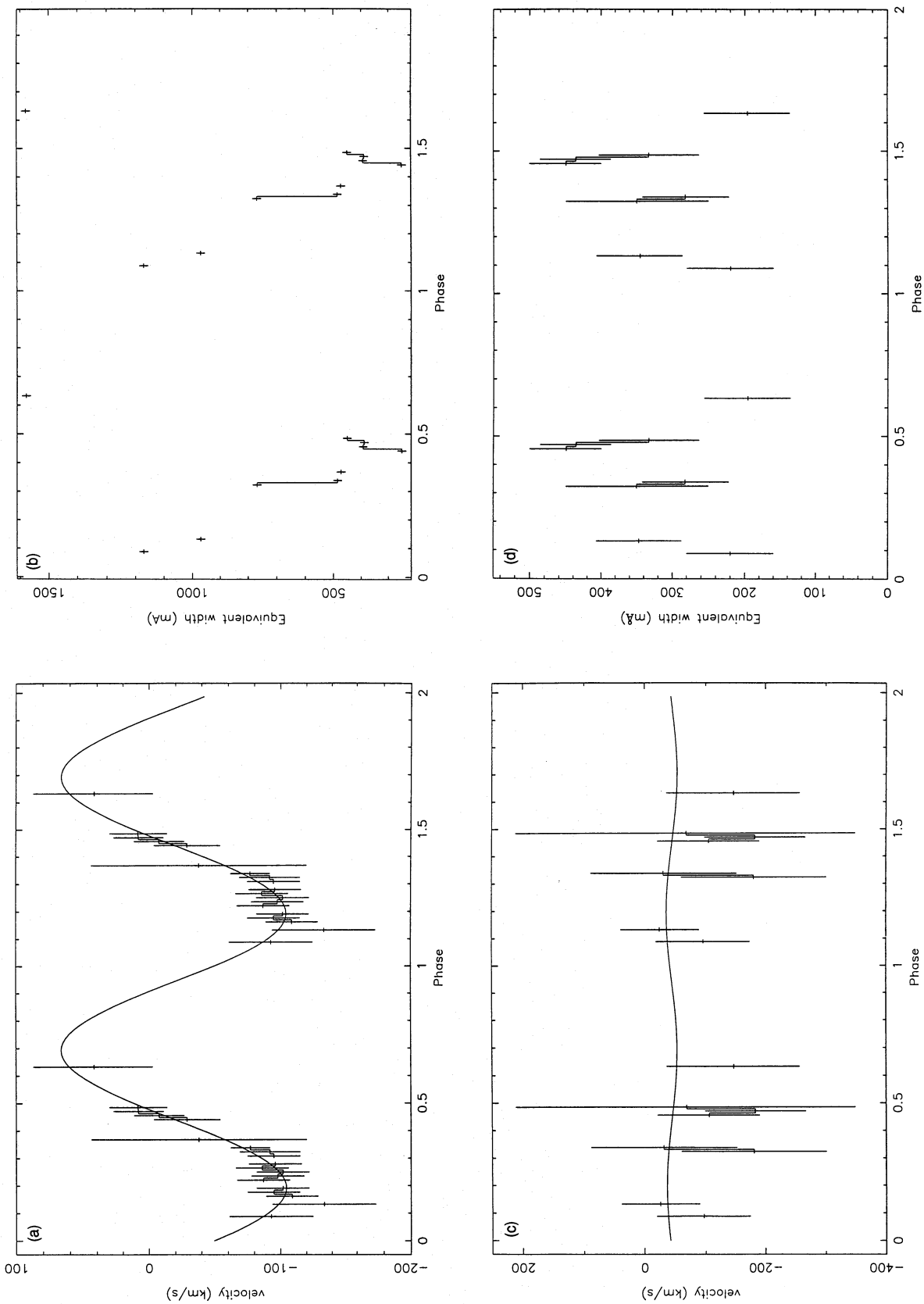

Figure 5. Radial velocities and line strengths as a function of phase for the 0.710 13-d period. (a) Emission-line radial velocities, (b) Hβ line equivalent widths, (c) He II 4686-Å absorption-line radial velocities, and (d) He absorption equivalent widths.

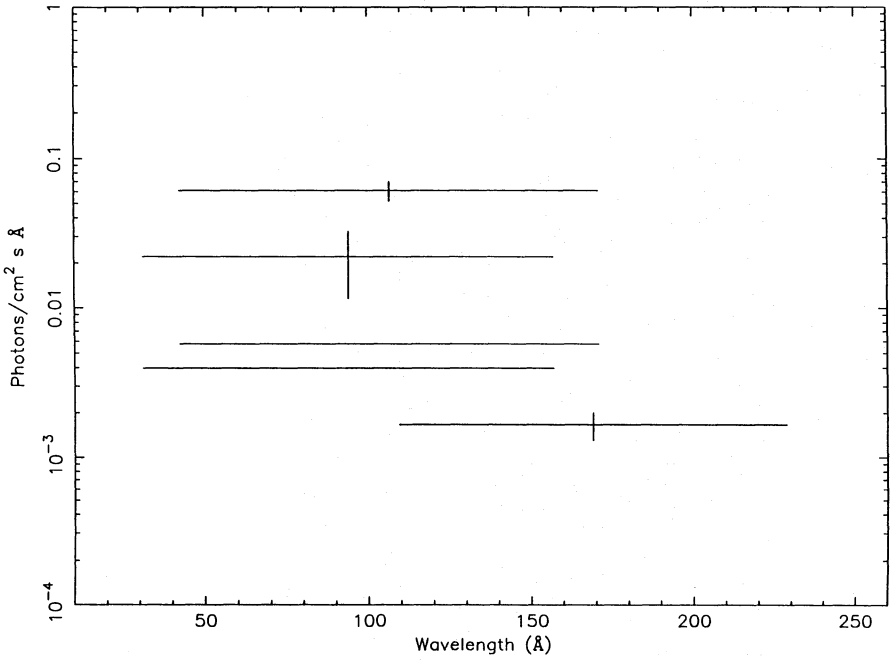

Figure 6. Comparison between the observed *ROSAT* PSPC and WFC S1 and S2 fluxes (error bars in increasing wavelength from left to right) and the corresponding predictions of a homogeneous model with $T=45\,800$ K, $\log g=7.66$ and $\log \mathrm{He/H}=-2.7$ (horizontal lines) for a value of the interstellar medium H I column (2.0×10^{18} cm^{-2}) which gives the best fit to the S2 data point.

observed S1 and PSPC values are about a factor of 10 higher than predicted (Fig. 6). Secondly, the He abundance was allowed to vary freely within the limits of the model grid to see whether the homogeneous model could fit with some other abundance of He. In fact, a good fit to the data is found when $\log \mathrm{He/H}=3.25$. The corresponding values of the other parameters are $T=48\,230$ K, $\log g=7.74$ and $N_{\mathrm{H}}=6.3\times10^{18}$ cm^{-2}. The 90 per cent error range on log He/H runs from -3.1 to -3.5. Clearly, the EUV and X-ray analysis is in some disagreement with the He abundance determined by the optical data. Of course, He is not necessarily the sole source of EUV/X-ray opacity in the white dwarf atmosphere. The *IUE* spectrum indicates that heavier elements (C IV and possibly Si III) are present. The observed features are unusually large and, with the relatively low EUV opacity observed in RE 2013+400, are likely to be mostly circumstellar, resulting from a wind–ISM shock, as suggested by Tweedy et al. (1993) in the analysis of RE 1016−053. However, if any of this material is photospheric, the required He abundance would be even lower than our simple analysis indicates.

5 DISCUSSION

The presence of narrow emission lines superimposed on the Balmer absorption spectrum of the white dwarf and the short, 0.71-d period we determine for this system from the radial velocity variations of the emission lines clearly show this system to be a pre-cataclysmic binary. The ≈ 6-$R_{\odot}$ separation of the system indicates that it almost certainly passed through a common-envelope phase when the white dwarf progenitor was a red giant. The relative phase of the radial velocity and emission-line flux is consistent with the expectation that the latter arises from reprocessing of the white dwarf EUV/X-ray flux incident on the red dwarf photosphere. Interestingly, we find that the red dwarf is an X-ray source in its own right, indicating a much higher level of activity in this companion star than in the red dwarfs of the similar systems Feige 24 and RE 1016−053. Both these objects are somewhat closer to the Earth than RE 2013+400, yet neither red dwarf is detected by the PSPC. An important factor may be the orbital period of these systems. The period of RE 1016−053 is unknown, but that of Feige 24 is ≈ 4 d, compared with the 0.71-d period we find for RE 2013+400. In the V471 Tau system the companion to the white dwarf is, at K2, much earlier than the red dwarf in RE 2013+400, but the period of ≈ 0.5 d is rather similar, and the companion is also an X-ray source and presumed to be rotating synchronously with the binary period. Hence we suggest that the enhanced activity in the RE 2013+400 red dwarf could, at least in part, be a result of rapid rotation caused by tidal interaction. One consequence of this would be that a fraction of the observed emission-line flux will probably be intrinsic to the red dwarf, constituting a base level that will not disappear at inferior conjunction, when the face illuminated by the white dwarf is away from us. Secondly, the red dwarf is likely to have a significant wind, like V471 Tau, from which the white dwarf could accrete material. In V471 Tau, a consequence of such accretion is the pulsation behaviour caused by rotational modulation of the X-ray/EUV dark and optically brightened polar regions (Barstow et al. 1992). The C IV and Si III features seen in the *IUE* spectrum may be a consequence of the interaction of an M dwarf wind with the white dwarf. Since RE 2013+400 is 10–20 times fainter in the EUV and X-ray than V471 Tau, the *ROSAT* survey light curves do not

have sufficiently high signal-to-noise ratio to search for similar pulsations, and we have not yet been able to carry out any high-speed astronomical photometry on this system. Clearly, such observations should be undertaken in the near future.

The spectral type of the RE 2013+400 primary is in keeping with an apparent tendency, reported by Tweedy et al. (1993), for the primary stars in pre-cataclysmic binaries to be DAO white dwarfs. However, the system is also a member of a small subgroup of these objects (Feige 24, V471 Tau and RE 1016−053; see above discussion) which are EUV/X-ray sources. Within this group, only RE 1016−053 is a DAO white dwarf and, so far, this and RE 2013+400 are the only such detections reported. In their detailed optical study of DAO white dwarfs, Bergeron et al. (1994) include both RE 1016−053 and 2013+400 in their sample, interpreting their spectra as arising from a homogeneous H+He atmosphere. They then explain the detection of these stars and the non-detection of all other known DAO white dwarfs by *ROSAT* (and *EUVE*) as arising from differences in heavy-element abundances in their photospheres. This is certainly a reasonable explanation, given that RE 1016−053 and 2013+400 are among the lowest temperature stars in the DAO group, but it is not necessarily the only possible interpretation.

The results of our combined optical and EUV/X-ray study show a possible stratification in the composition and structure of the white dwarf in RE 2013+400 which is not revealed by optical observations alone (cf. Bergeron et al. 1994). Analysis of the optical spectra yields a temperature ($\approx$47 000 K) and log gravity ($\approx$7.7) which are consistent with the results of Bergeron et al. (1994, $T=47\,800\pm2400$ K, $\log g=7.69\pm0.16$ and $\log \mathrm{He/H}=-2.62\pm0.63$). The largest of our He abundance measurements also agrees with theirs. However, we have two additional pieces of evidence which add to the picture. First, the observed variability in He absorption-line strength with orbital phase, which seems most likely to be a result of infilling of the absorption line with a variable emission component, suggests that the values of the He abundance that we and Bergeron et al. quote may only be lower limits. Secondly, and more important, are the results of the EUV/X-ray analysis which appear to require the He abundance to be 1–2 orders of magnitude lower than the optical data imply. Initially, we need to treat this result with a certain amount of caution, since we are aware of some anomalies in fitting the He II line profiles in DAO white dwarfs (Werner, private communication). However, tests of different He II line-broadening formalisms in the models used here indicate that any possible systematic errors in determining the respective He abundances are likely to be smaller than the differences observed. How can we resolve this problem? The simplest explanation is to take all measurements at their face value, and interpret the result as an abundance gradient in the star. Often it is assumed that observations in the EUV/X-ray regions of the spectrum probe deeper into the atmosphere. However, when significant quantities of He are present, this is no longer true. Indeed, the EUV/X-ray continuum flux is formed higher in the atmosphere than the optical lines. Hence our result would be in keeping with the idea that the atmosphere of the star is stratified in some way, but with a weaker gradient than is present in simple equilibrium models. Alternatively, since the EUV/X-ray, UV and optical observations are well separated in time, we might consider that the He abundance is varying on a long time-scale, being particularly low when the star was observed by *ROSAT*. While we cannot completely rule out this possibility, it seems unlikely when the same He abundance is measured from the SO and INT data sets, which are separated by several months.

It is interesting that the only DAO white dwarfs detected by *ROSAT* are in binary systems. Most of the white dwarfs in the Bergeron et al. (1994) sample are isolated objects, and the presence of a homogeneous mixture of He requires an as yet unknown mechanism to prevent the He settling out of the atmosphere under the influence of gravity. Bergeron et al. (1994) suggest that mass loss may be the cause, but there is, at the moment, no theoretical work to test this proposition. In RE 2013+400 and 1016−053, an alternative possibility is that He could be accreted from a companion wind. We know of at least one system, V471 Tau, where this is happening (e.g. Barstow et al. 1992), and there is a strong indication, from the work presented here, that the red dwarf in RE 2013+400 also has a wind. Photospheric He has not been detected in the V471 Tau system but, as the magnetic field confines the accretion to small polar caps on the white dwarf, it may well be more difficult to find spectroscopically. If accretion is the source of He in RE 2013+400, then the detection of this star (and by association RE 1016−053) at EUV and X-ray wavelengths could be a consequence of its particular structure, rather than a lower abundance of heavy elements. A knowledge of whether or not the atmospheric structure of RE 2013+400 might be typical of the wider class of DAO white dwarfs is crucial. If a He abundance gradient is present in all of these stars, this could be an important indicator as to the supporting mechanism and, at the very least, it must be explained by any proposed model.

6 CONCLUSION

Our multiwavelength observations have revealed much of the nature of the *ROSAT* discovery RE 2013+400, but have raised a number of unanswered questions. It is a pre-cataclysmic binary, the white dwarf having a temperature of $\approx$47 000 K and $\log g\approx7.7$. The system is quite similar to the pre-CVs Feige 24 and RE 1016−053 in its detection as an EUV/X-ray source and also in having an M dwarf secondary. However, its 0.71-d period is much shorter than Feige 24, at least, and the M dwarf has a level of intrinsic activity much more like that of the K2 dwarf in the pulsating/eclipsing binary V471 Tau. We suggest that a search for similar pulsations in RE 2013+400 should be carried out with high-speed photometry.

Possibly the most intriguing feature is the detection of He in the optical line-forming region of the photosphere but with much too low an abundance, if indeed there is any present, to be found in the region where the EUV/X-ray continuum is formed. This could be a consequence of the binary nature of the object, if the source of the He is accretion from a companion wind. Alternatively, if RE 2013+400 is typical of many DAO white dwarfs (note that it is included in the sample studied by Bergeron et al. 1994), the atmospheric structure we appear to have observed could be an important clue to the mechanism that prevents the He sinking out of the photosphere under the influence of gravity, as predicted by theory (Vennes et al. 1988).

In our interpretation, with the evidence we have, any variation in the strength of the He II 4686-Å absorption feature has been ascribed to infilling of the feature with an emission component of varying strength. We do not have data of sufficiently high signal-to-noise ratio or spectral resolution to examine the alternative possibility that the He abundance may be truly changing. If the He is accreted, it is not necessarily distributed uniformly over the surface of the white dwarf. An inhomogeneous surface distribution of the material may be partly responsible for some of the abundance effects we have seen.

It is important that we answer these questions; to do this we require further observations of this system, but with higher signal-to-noise ratio, better spectral resolution and improved temporal coverage than the data in this paper. In addition to more detailed studies of RE 2013+400, the work included in this paper needs to be extended to other pre-CV systems and isolated DAOs to learn more about the structure and composition of this important group of white dwarfs.

ACKNOWLEDGMENTS

MAB, MRB and MCM are supported by the PPARC, UK. TAF, JBH and RWT are supported by NASA grants. SS and GW are supported by NSF grant AST 93-47714. GW also acknowledges support from SERC and the Alexander von Humboldt-Stiftung. We thank the referee, Dr Pierre Bergeron, for his important comments on the original version of this paper. We are also grateful to Dr Matt Wood for the use of his evolutionary models. The data reductions and analyses were performed with Starlink, NOAO and NASA HEASARC software.

Our paper is based on observations made with the *ROSAT* observatory (operated by the Max-Planck-Institut für Extraterrestriche Physik), the Steward Observatory 2.3-m telescope, operated by the University of Arizona, the 2.5-m Isaac Newton Telescope, operated on the island of La Palma by the Royal Greenwich Observatory in the Spanish Observatorio del Roque de los Muchachos of the Instituto de Astrofísica de Canarias, and the 2.4-m Hiltner Telescope at the McGraw-Hill Observatory, operated jointly by the University of Michigan, Dartmouth College and Massachusetts Institute of Technology.

REFERENCES

Barstow M. A., Schmitt J. H. M. M., Clemens J. C., Pye J. P., Denby M., Harris A. W., Pankiewicz G. S., 1992, MNRAS, 255, 369
Barstow M. A. et al., 1993a, MNRAS, 264, 16
Barstow M. A., Hodgkin S. T., Pye J. P., King A. R., Fleming T. A., Holberg J. B., Tweedy R. W., 1993b, in Barstow M. A., ed., White Dwarfs: Advances in Observation and Theory, Kluwer, Dordrecht, p. 433
Barstow M. A. et al., 1994, MNRAS, 270, 499
Bergeron P., Saffer R. A., Liebert J., 1992, ApJ, 394, 228
Bergeron P., Wesemael F., Beauchamp A., Wood M. A., Lamontagne R., Fontaine G., Liebert J., 1994, ApJ, 432, 305
Bowyer C. S. et al., 1994, ApJS, 93, 569
Chayer P., Fontaine G., Wesemael F., 1991, in Vauclair G., Sion E., eds, White Dwarfs. Kluwer, Dordrecht, p. 249
Cooke B. A. et al., 1992, Nat, 355, 61
Fleming T. A., Molendi S., Maccacaro T., Wolter A., 1994, AJ, in press
Fulbright M. S., Liebert J. W., Bergeron P., Green R. F., 1993, ApJ, 406, 240
Green R. F., Schmidt M., Liebert J. W., 1986, ApJS, 61, 305
Jomaron C., Branduardi-Raymont G., Mason K. O., Naylor T. T., Hassall B. J. M., Watson M. G., Hodgkin S. T., Bromage G. E., 1993, MNRAS, 264, 219
King A. R., 1989, QJRAS, 29, 1
Koester D., 1991, in Michaud G., Tutukov A., eds, Proc. IAU Symp. 145, Evolution of Stars: The Photospheric Abundance Connection. Kluwer, Dordrecht, p. 435
Livio M., Soker N., 1988, ApJ, 329, 764
Malina R. F. et al., 1994, AJ, 107, 751
Mason K. O. et al., 1991, Vistas Astron., 34, 343
Pounds K. A. et al., 1993, MNRAS, 260, 77
Ritter H., 1986, A&A, 169, 139
Shafer R. A., Haberl F., Arnaud K. A., Tennant A. F., 1991, ESA TM-09. ESA Publ. Division, Noordwijk
Sion E. M., Holberg J. B., Barstow M. A., Kidder K. M., 1994, PASP, in press
Thorstensen J. R., Vennes S., 1994, BAAS, 26, 1377
Thorstensen J. R., Charles P. A., Margon B., Boywer S., 1978, ApJ, 223, 260
Tweedy R. W., Holberg J. B., Barstow M. A., Bergeron P., Grauer A. D., Liebert J., Fleming T. A., 1993, AJ, 105, 1938
Vauclair G., 1989, in Wegner G., ed., White Dwarfs. Springer-Verlag, Berlin, p. 176
Vennes S., Thorstensen J. R., 1994, AJ, 108, 1881
Vennes S., Pelletier C., Fontaine G., Wesemael F., 1988, ApJ, 331, 876
Vennes S., Chayer P., Fontaine G., Wesemael F., 1989, ApJ, 336, L25
Wood M. A., 1992, ApJ, 386, 539